The Canadian Mineralogist
Vol. 40, pp. 1675-1686 (2002)

WALKERITE, A NEW BORATE MINERAL SPECIES IN AN EVAPORITIC SEQUENCE FROM SUSSEX, NEW BRUNSWICK, CANADA

JOEL D. GRICE[§], ROBERT A. GAULT AND JERRY VAN VELTHUIZEN[†]

Research Division, Canadian Museum of Nature, P.O. Box 3443, Station D, Ottawa, Ontario K1P 6P4, Canada

ALLEN PRATT

CANMET, 555 Booth Street, Ottawa, Ontario K1A 0G1, Canada

ABSTRACT

Walkerite, ideally $Ca_{16}(Mg,Li,\square)_2[B_{13}O_{17}(OH)_{12}]_4Cl_6 \bullet 28H_2O$, is a new mineral species from the Potash Corporation of Saskatchewan (New Brunswick Division) mine at Penobsquis, near Sussex, Kings County, New Brunswick. It occurs in the Upper Halite Member of the Windsor Group evaporites, associated with halite, hydroboracite, hilgardite, volkovskite, boracite, szaibelyite, a mica-group mineral and anhydrite. The crystals of walkerite are colorless to white, fibrous to acicular, commonly forming bundles of fibers to 7 mm in length. The crystals are transparent to translucent, with a vitreous luster and a white streak. It is soft (Mohs hardness of 3), brittle with no apparent cleavage, but with a splintery fracture along [001]. Walkerite is biaxial positive, α 1.516 ± 0.002, β 1.532 ± 0.002 and γ 1.554 ± 0.002 (for λ = 590 nm); $2V_{meas.}$ = 82(3)°, $2V_{calc.}$ = 82°. There is no dispersion and no pleochroism. Optical orientation: X = **a**, Y = **b** and Z = **c**. It is orthorhombic, space group *Pba*2, with unit-cell parameters refined from powder data: *a* 15.52(1), *b* 22.74(1), *c* 8.761(4) Å, *V* 3091(2) Å^3 and Z = 1. The strongest six powder-diffraction lines [*d* in Å(*I*)(*hkl*)] are: 12.820(100)(110), 7.785(80)(200), 6.319(40)(121), 5.649(30)(211), 3.176(30)(170) and 2.570(30)(461,550). Electron-microprobe analyses, a thermogravimetric analysis and induced coupled plasma – mass spectrometry results, supported by crystal-structure analysis, infrared-absorption spectrometry and secondary-ion mass spectrometry, yielded Li_2O 0.12, Na_2O 0.13, K_2O 0.07, CaO 23.05, FeO 0.32, MgO 0.58, Cl 4.91, B_2O_3 47.17 and H_2O 25.48, O = Cl –1.11, total 100.72 wt.%. The empirical formula based on 150 anions, is $(Ca_{15.60}Na_{0.16}K_{0.06})_{\Sigma 15.82}(Mg_{0.55}Li_{0.31}Fe_{0.17})_{\Sigma 1.03}$ $B_{51.43}O_{68}(OH)_{48}[Cl_{5.26}(OH)_{0.74}]_{\Sigma 6.00}$ $H_{2.53} \bullet 28H_2O$; the idealized formula is presented above. The calculated density (from the empirical formula) is 2.05 g/cm^3, and the measured density is 2.07 g/cm^3. The structure has been refined to R = 0.040. The highly corrugated sheets of borate polyhedra are cross-linked by Ca and Mg polyhedra. The Cl atoms and H_2O groups are located within the ovoid channels. The structure is compared to that of other complex borates, such as penobsquisite and pringleite.

Keywords: walkerite, new mineral species, crystal structure, borate, polymerization, evaporite, Sussex, New Brunswick.

SOMMAIRE

La walkerite, dont la formule idéale serait $Ca_{16}(Mg,Li,\square)_2[B_{13}O_{17}(OH)_{12}]_4Cl_6 \bullet 28H_2O$, est une nouvelle espèce minérale découverte à la mine de la Potash Corporation of Saskatchewan (division du Nouveau-Brunswick), à Penobsquis, près de Sussex, comté de Kings, au Nouveau-Brunswick. Elle se trouve dans l'unité appelée Upper Halite, membre du Groupe de Windsor contenant des évaporites, où elle est associée à halite, hydroboracite, hilgardite, volkovskite, boracite, szaibelyite, un minéral du groupe des micas et anhydrite. Les cristaux de walkerite sont incolores à blanc, fibreux à aciculaires, en essaims atteignant 7 mm en longueur. Les cristaux sont transparents à translucides, avec un éclat vitreux et une rayure blanche. Il s'agit d'un minéral tendre (dureté de Mohs 3), cassant, sans clivage apparent, mais avec une fracture en échapes le long de [001]. La walkerite est biaxe positive, α 1.516 ± 0.002, β 1.532 ± 0.002 et γ 1.554 ± 0.002 (λ = 590 nm); $2V_{mes.}$ = 82(3)°, $2V_{calc.}$ = 82°. Il n'y a pas de dispersion ou de pléochroïsme. L'orientation optique est: X = **a**, Y = **b** et Z = **c**. Le minéral est orthorhombique, groupe spatial *Pba*2, avec les paramètres réticulaires suivants, affinés à partie du spectre de diffraction obtenu sur poudre: *a* 15.52(1), *b* 22.74(1), *c* 8.761(4) Å, *V* 3091(2) Å^3 et Z = 1. Les six raies les plus intenses [*d* en Å(*I*)(*hkl*)] sont: 12.820(100)(110), 7.785(80)(200), 6.319(40)(121), 5.649(30)(211), 3.176(30)(170) et 2.570(30)(461,550). Les données obtenues à la microsonde électronique, les résultats d'une analyse thermogravimétrique et d'une autre avec plasma à couplage inductif et spectrométrie de masse, étayés par une détermination de la structure cristalline, un spectre d'absorption infrarouge et la spectrométrie de masse sur ions secondaires, ont donné Li_2O 0.12, Na_2O 0.13, K_2O 0.07, CaO 23.05, FeO 0.32, MgO 0.58, Cl 4.91, B_2O_3 47.17 et H_2O 25.48, O = Cl –1.11, pour

§ *E-mail address*: jgrice@mus-nature.ca
† Deceased

un total de 100.72% (poids). La formule empirique, fondée sur 150 anions, serait $(Ca_{15.60}Na_{0.16}K_{0.06})_{\Sigma 15.82}(Mg_{0.55}Li_{0.31}Fe_{0.17})_{\Sigma 1.03}B_{51.43}O_{68}(OH)_{48}[Cl_{5.26}(OH)_{0.74}]_{\Sigma 6.00}H_{2.53}\bullet 28H_2O$; elle est exprimée de façon idéale ci-haut. La densité calculée (pour la formule empirique) est 2.05 g/cm^3, et la densité mesurée est 2.07 g/cm^3. Nous en avons affiné la structure jusqu'à un résidu *R* de 0.040. Les feuillets de polyèdres de borate sont fortement ondulants, et interliés par des polyèdres à Ca et Mg. Les atomes Cl et les groupes H_2O sont situés dans des canaux ovoïdes. Nous comparons la structure à celle d'autres borates complexes, tels la penobsquisite et la pringléite.

(Traduit par la Rédaction)

Mots-clés: walkerite, nouvelle espèce minérale, structure cristalline, borate, polymérisation, évaporite, Sussex, New Brunswick.

Introduction

Walkerite is the latest in a series of new borate minerals to be described from the evaporite deposits of southern New Brunswick. The others include trembathite (Burns *et al.* 1992), pringleite and ruitenbergite (Roberts *et al.* 1993), penobsquisite (Grice *et al.* 1996) and brianroulstonite (Grice *et al.* 1997). Walkerite was discovered during a systematic examination of residue obtained from the dissolution of halite drill-core from the mine operated by the Potash Corporation of Saskatchewan (New Brunswick Division) (formerly Potash Company of America), 5 km east of Penobsquis, Sussex area, Cardwell Parish, Kings County, New Brunswick. Fibrous crystals were noted in the residue. Subsequent X-ray and electron-microprobe analyses clearly indicated that this was an unknown phase. The data presented here establish this mineral as a new species.

Walkerite is named in honor of Thomas Leonard Walker (1867–1942) (Fig. 1), for his contributions to mineralogy in general and to the study of borates from the Minas Basin, Nova Scotia, in particular. The borate minerals he studied are from the same formation as that containing the walkerite. Dr. Walker received his Ph.D. from the University of Leipzig in 1896 and continued his studies in crystallography at the University of Heidelberg. He was appointed Assistant Superintendent of the Geological Survey of India in 1897, returning to Canada in 1901 to become Professor of Mineralogy and Petrography at the University of Toronto. He was appointed as the first Director of the Royal Ontario Museum, Toronto, in 1913. He was a founding member and former President of the Geological Society of America, and a fellow and member of many geological societies in Canada, the United States and Great Britain. As well, he established the journal *Contributions to Canadian Mineralogy*, the predecessor of *The Canadian Mineralogist*. He received an honorary Doctor of Science degree from the University of Toronto and the Flavelle Medal for his important contributions to mineralogical sciences from the Royal Society of Canada. The new mineral and the name have been approved by the Commission on New Minerals and Mineral Names, IMA (IMA 2002–051). Cotype material is housed in the collection of the Canadian Museum of Nature, Ottawa under catalogue numbers CMNMC 83379 and CMNMC 83380.

Occurrence

Walkerite occurs in the lower third of the Upper Halite Member, within a thick sequence of evaporites in the Windsor Group. The stratigraphy and geological setting of the evaporite deposits were described by Roulston & Waugh (1981). The evaporites are Mississippian in age and occur in the Moncton sub-basin, part of the Fundy geosyncline, a northeasterly trending depositional trough extending through southern New Brunswick, Nova Scotia and western Newfoundland.

FIG. 1. Thomas Leonard Walker (1867–1942).

The presence of borate minerals from two potash mines in the Penobsquis–Sussex area of New Brunswick was first noted in the early 1980s in residue from the drilling operations. They were subsequently identified in the mining companies' laboratories and at various institutions (Roulston & Waugh 1981). The list of borate minerals compiled from these earlier investigations and from our study includes boracite, brianroulstonite, colemanite, congolite, danburite, ginorite, hilgardite-1*A*, hilgardite-4*M*, howlite, hydroboracite, inyoite, penobsquisite, priceite, pringleite, ruitenbergite, strontioginorite, szaibelyite, trembathite, tyretskite, veatchite, volkovskite and walkerite. Other minerals found with the borate assemblage include anhydrite, sellaite, fluorite, nickeline, pyrite, chalcopyrite, sphalerite, halite, sylvite, microcline, diopside, quartz, a mica-group mineral, a clay-group mineral, hematite, limonite, magnesite, calcite, dolomite, monohydrocalcite and malachite. Organic material is present in several sections of the core.

Walkerite was found in drill core from the Potash Corporation of Saskatchewan mine, and is intimately associated with halite, hydroboracite, hilgardite, volkovskite, boracite, szaibelyite, the mica-group mineral and anhydrite. Approximately 100 single crystals with a total approximate weight of 30 mg were separated, along with numerous bundles of fibers.

Physical and Optical Properties

Walkerite exhibits a fibrous to bladed morphology (Fig. 2), and the fibers commonly occur in bundles (Fig. 3). They are elongate on [001], with bundles up to 7 mm in length and individual acicular crystals to 2 × 0.05 mm. Forms observed were pinacoids {100} and {010} and pedion {001}. No twinning was observed. The crystals are transparent to translucent, colorless to white, with a white streak and vitreous luster. Walkerite shows no fluorescence with either short-wave or long-wave ultraviolet light. It has an approximate hardness of 3 (Mohs scale), is brittle, with no apparent cleavage, but with a splintery fracture along [001]. The density, 2.07 ± 0.03 g/cm^3, was measured by suspension in bromoform and agrees well with the calculated density, 2.05 g/cm^3.

Walkerite is biaxial positive, with indices of refraction α 1.516 ± 0.002, β 1.532 ± 0.002 and γ 1.554 ± 0.002 (for λ = 590 nm); $2V_{meas.} = 82(3)°$, $2V_{calc.} = 82°$. There is no dispersion and no pleochroism. The optical orientation is X = **a**, Y = **b** and Z = **c**. A Gladstone–Dale calculation gives a compatibility index of –0.038, which is regarded as excellent (Mandarino 1981).

Chemical Composition

Electron-microprobe analysis

The chemical analyses were performed on a JEOL 733 electron microprobe in wavelength-dispersion (WD) mode using Tracor Northern 5500 and 5600 automation. Data reduction was done with a PAP routine in XMAQNT (C. Davidson, CSIRO, pers. commun.). The operating voltage was 15 kV, and the beam current was 20 nA. The beam diameter varied from 20 to 40 μm. The following standards were used: albite (Na$K\alpha$), rubidian microcline (K$K\alpha$), danburite (Ca$K\alpha$), dolomite

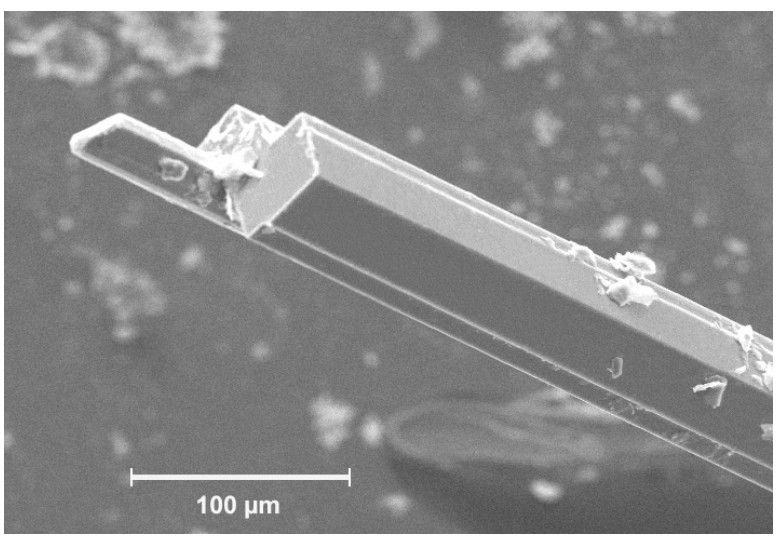

FIG. 2. Scanning electron micrograph of walkerite.

(Mg$K\alpha$), almandine (Fe$K\alpha$) and tugtupite (Cl$K\alpha$). Several 100 s energy-dispersion (ED) scans indicated no elements with Z > 8 other than those reported here. Manganese, Sr and F were sought but not detected. Data for all elements in the samples were collected for 25 s or 0.50% precision, whichever was attained first. Eighteen electron-microprobe analyses were performed on different grains, including the one selected for analysis of the structure; the average (with ranges) is reported here. The concentrations of Li and B were established by induced coupled plasma – mass spectrometry (ICP–MS) and confirmed by secondary-ion mass spectrometry (SIMS). The presence of H_2O was confirmed by infrared-absorption spectrometry (IR), and its concentration was established by thermogravimetric analysis (TGA).

The chemical composition is: Li_2O 0.12, Na_2O 0.13 (0–1.05), K_2O 0.07 (0–0.26), CaO 23.05 (21.52–24.79), FeO 0.32 (0.16–0.44), MgO 0.58 (0.16–0.88), Cl 4.91 (3.33–5.68), B_2O_3 47.17 and H_2O 25.48, O = Cl –1.11, total 100.72 wt.%. The empirical formula based on 150 anions, as deduced from the crystal-structure analysis, is $(Ca_{15.60}Na_{0.16}K_{0.06})_{\Sigma 15.82}(Mg_{0.55}Li_{0.31}Fe_{0.17})_{\Sigma 1.03}B_{51.43}O_{68}(OH)_{48}[Cl_{5.26}(OH)_{0.74}]_{\Sigma 6.00}H_{2.53}\bullet 28H_2O$ or, ideally, $Ca_{16}(Mg,Li,\square)_2[B_{13}O_{17}(OH)_{12}]_4Cl_6\bullet 28H_2O$.

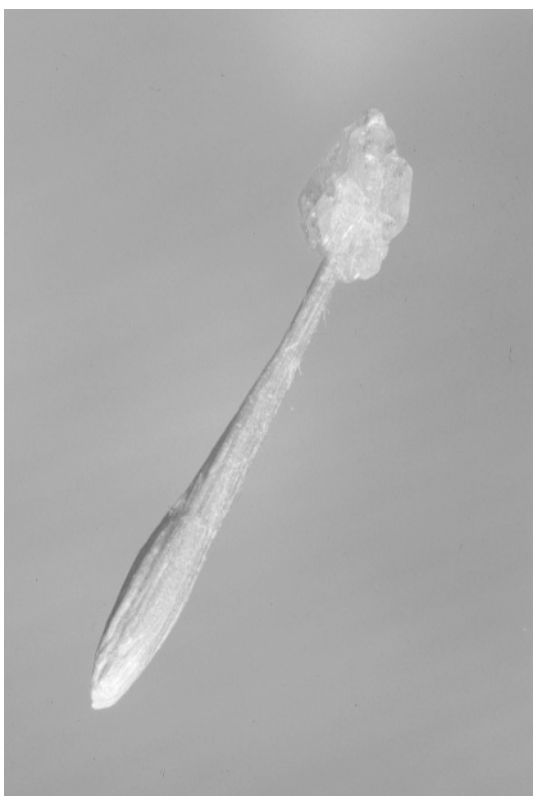

FIG. 3. Photograph of a bundle of walkerite fibers 6 mm in length, capped by hilgardite. Photograph by Q. Wight. Also in color on page 1685.

Infrared analysis

The infrared spectrum of walkerite (Fig. 4) was obtained using a Bomem Michelson MB–120 Fourier-transform infrared spectrometer with a diamond-anvil cell as a microsampling device. The broad peak centered in the 3409 cm^{-1} region, the O–H stretching frequency, indicates the presence of OH^- anions or H_2O groups. The broadness and fine structure of the peak indicate a variety of distinct OH or H_2O groups in the structure. The peak centered at 1650 cm^{-1} is attributed to H–O–H bending, which confirms the presence of H_2O groups. Comparing the remaining complex part of the spectrum to spectra given in Farmer (1974), the following frequency regions are assigned modes: 1324 and 1235 cm^{-1}: asymmetric stretching in $[BO_3]$, 1100–900 cm^{-1}: asymmetric stretching in $[BO_4]$ and symmetric stretching in $[BO_3]$, and 709 cm^{-1}: symmetric stretching in (BO_4).

Thermogravimetric analysis

TGA was performed on a Mettler TG50 module linked to a Mettler M3 microbalance. The purge gas was dry nitrogen, with a flow rate of 100 mL/min. One sample weighing 4.58 mg was ground to a fine powder and heated from 30° to 1000°C at a rate of 25°C/min.

The weight loss occurred in five distinct steps, which are interpreted as follows: [1] 33–147°C, the loss of 28 H_2O groups, 12.90 wt.%, [2] 147–286°C, the loss of 28 OH groups, 7.10 wt.%, [3] 286–575°C, the loss 20 OH groups, 5.48 wt.%, [4] 575–781°C, the loss of H-bonded Cl, 1.80 wt.%, and [5] 781–890°C, the loss of H-bonded Cl, 3.12 wt.%.

Induced coupled plasma – mass spectrometry and secondary-ion mass spectrometry

Positive SIMS mass spectra were acquired using a 12.5 kV, 82 nanoampere O^{--} primary ion beam. The SIMS instrument is a modified Cameca IMS 4f housed at the CANMET Materials Technology Laboratory, Ottawa. The sample was prepared for analysis as a standard polished section 2.5 cm in diameter. The polished section was carbon-coated to make it conductive. The O^- primary ion beam was rastered over an area 250 × 250 μm, and SIMS data were collected from a spot in the center of the raster area (crater) 150 μm in diameter. Mass spectra collected from the sample were characterized by peaks near 6.0 and 7.0 atomic mass units (*amu*). These peaks are respectively interpreted to originate from $^6Li^+$ and $^7Li^+$. Substantial mass-interferences for $^6Li^+$ and $^7Li^+$ were not expected, and no special mass-filtering techniques were applied.

A Perkin–Elmer Sciex Elan 6100 DRC housed at the CANMET Mining and Mineral Sciences Laboratory, Ottawa, was used for the ICP–MS experiment; 898 μg of sample was dissolved in 2.00 mL of ultra-high-purity concentrated nitric acid. To conduct the ICP–MS measurements, the solution volume was increased to 10.18 mL, and the solution was then analyzed for Li, B, Mg and Ca. Quantification was undertaken using research-grade reference solutions. The amount of B_2O_3, 47.17 wt.%, compares well with the ideal amount, 46.08 wt.% expected from the crystal-structure analysis. The ICP–MS results for Mg and Ca fall well within the ranges determined with an electron microprobe.

X-Ray Crystallography and Crystal-Structure Determination

X-ray precession photographs show walkerite to be orthorhombic, with possible space-groups *Pba*2 (space group #32) and *Pbam* (space group #55) for a setting choice of $c < a < b$. X-ray powder-diffraction data collected with a 114.6 mm diameter Debye–Scherrer camera with Cu*K*α (Ni-filtered) radiation are given in Table 1. For purposes of indexing, a powder pattern was calculated using the atom coordinates determined in the crystal-structure analysis to evaluate whether or not an *hkl* plane contributed to a reflection.

The single crystal of walkerite used for the collection of X-ray intensity data (part of the cotype specimen) measures 0.30 × 0.10 × 0.06 mm. Intensity data were collected on a fully automated Siemens *P*4 four-circle diffractometer equipped with a CCD detector and operated at 50 kV, 40 mA, with graphite-monochromated Mo*K*α radiation. Almost a full sphere of intensity data was collected up to 2θ = 60° using 60 s frames and a crystal-to-detector distance of 40 mm. With these operating conditions, no decrepitation was evident in the final analysis of the reflections used as intensity standards. Information relevant to the data collection and structure determination is given in Table 2. The three-dimensional data were reduced for Lorentz, polarization, and background effects, and multiply-measured reflections were averaged using the

TABLE 1. WALKERITE: X-RAY POWDER-DIFFRACTION DATA

$I_{est.}$	$d_{obs.}$ (Å)	$d_{calc.}$ (Å)	*hkl*	$I_{est.}$	$d_{obs.}$ (Å)	$d_{calc.}$ (Å)	*hkl*
10	12.820	12.812	110	<1	2.201	2.199	0$\bar{1}$01
8	7.785	7.757	200	<1	2.159	2.158	443
2	6.805	6.806	130	1	2.085	2.085	134
4	6.319	6.333	121	2	2.020	2.019	183
3	5.649	5.627	211	1	1.956		
<1	5.078	5.042	310	1	1.908		
<1	4.569	4.556	141	1	1.877		
<1	4.366	4.370	311, 150	<1	1.841		
2	4.137	4.146	321	1	1.792		
1	3.884	3.878	400	<1	1.752		
1	3.508	3.504	411	1	1.721		
1	3.392	3.392	161, 421	<1	1.697		
3	3.176	3.177	170	<1	1.669		
<1	3.081	3.091	152	<1	1.651		
<1	2.986	2.995	270	<1	1.622		
<1	2.896	2.901	402, 412	1	1.592		
1	2.781	2.782	123	<1	1.548		
<1	2.704	2.713	213	<1	1.520		
3	2.570	2.571	610, 550	<1	1.495		
1	2.478	2.481	323	<1	1.478		
2	2.413	2.411	333	<1	1.462		
<1	2.322	2.321	413	<1	1.437		
<1	2.288	2.287	163	<1	1.416		

114.6 mm Debye–Scherrer camera, Cu*K*α radiation, visually estimated intensities. Indexing based on cell: a 15.52(1), b 22.74(1), c 8.761(4) Å, V 3091(2) Å^3.

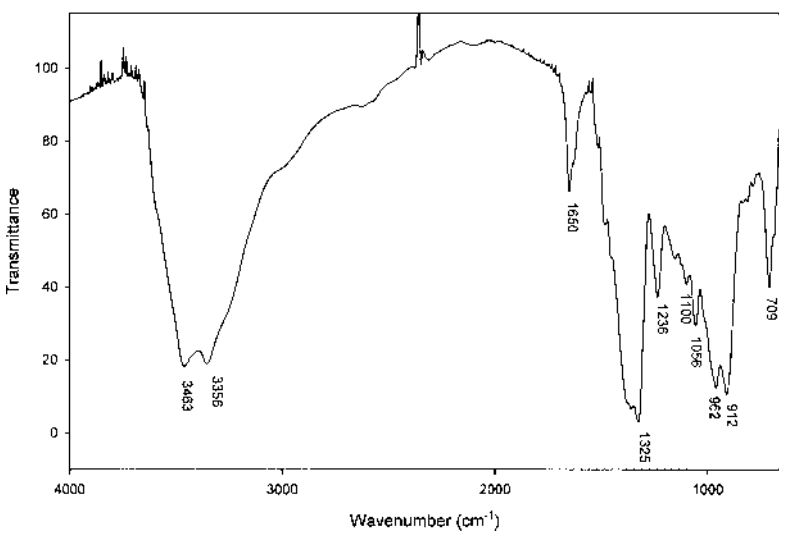

FIG. 4. Infrared spectrum of walkerite.

Bruker program SAINT. An empirical ellipsoid-absorption correction was done on the basis of 5168 reflections and reduced the merging R of this dataset from 5.47% before the absorption correction to 4.20% after the absorption correction.

All calculations were done with the Siemens SHELXTL Version 5.03 system of programs, which incorporates scattering factors of neutral atoms taken from the International Tables for X-ray Crystallography (Ibers & Hamilton 1974). Assigning phases to a set of normalized structure-factors gave a mean value $|E^2 - 1|$ of 0.777, suggesting the noncentrosymmetric space-group *Pba*2. The *E*-map coordinates were assigned with appropriate scattering curves to four *Ca* sites, two *Cl* sites and twenty *O* sites. Through a series of difference-Fourier maps in subsequent refinements, a complete model of the structure was attained. With all of the sites assigned the correct scattering-curves, the model refined to $R = 0.072$ with isotropic displacement-factors. In the final least-squares refinement, all atom positions were refined with anisotropic displacement-factors to final residuals of $R = 0.042$ and $R_w = 0.041$ for observed intensity data. The weighting scheme is inversely proportional to $\sigma^2(F)$. The addition of an isotropic extinction-correction did not improve the refinement, nor was there any evidence of twinning. The maximum and minimum electron-densities in the final cycle of refinement were +0.45 and –0.39 $e^-/Å^3$. The final positional and anisotropic displacement-parameters are given in Table 3, and selected bond-lengths and angles, in Table 4. Tables listing the observed and calculated structure-factors as well as the anisotropic displacement-parameters may be obtained from the Depository of Unpublished Data, CISTI, National Research Council of Canada, Ottawa, Ontario K1A 0S2, Canada.

Description of the Structure

The crystal structure of walkerite is a complex corrugated borate sheet structure consisting of thirteen crystallographically distinct borate polyhedra, six of which are triangular [(BO_3) groups] and seven of which are tetrahedral [(BO_4) groups]. There are two types of triangular coordination, the common [BO_3] and the much rarer [$BO_2(OH)$]. There are three types of tetrahedral coordination, [BO_4], [$BO_3(OH)$] and [$BO_2(OH)_2$] (Table 4). Those O atoms bonded to two B atoms are O^{2-} anions, whereas O atoms bonded to one B atom are part of an $(OH)^-$ group. There are no H_2O groups bonded to B, three groups are bonded to Ca and the remaining four H_2O groups are H-bonded to other H_2O groups or OH groups. The Cl atoms are H-bonded to H_2O groups. Three of the *Ca* atom sites have [9]-coordination, whereas a fourth (atom site *Ca*3) has [8]-coordination. The *Mg* site is unique in this structure, with site multiplicity and Wyckoff letter 2*a*. It has pseudotetrahedral coordination (Table 4) with two Mg–OH bond lengths of 2.08 Å and two of 1.86 Å. This site is key to the cross linkage of the sheets. Using the scattering curve for Mg, the site occupancy refines to 0.252(4) (ideally ½). This corresponds to 6.1(1) e^-, *i.e.*, approximately 1 Mg in this 2-fold site. On the basis of this half-occupancy of the *Mg* site, we investigated the possibility of Li-for-Mg substitution. Li commonly has tetrahedral coordination, with Li–O bond lengths in the range 1.86–2.05 Å, as given in Table 4.1.1 in the International Tables for X-ray Crystallography (Ondik & Smith 1968). Similarly Fe^{3+} can have tetrahedral coordination, with Fe–O bond lengths in this range. In the empirical formula presented above, this *Mg* site was said to contain $(Mg_{0.55}Li_{0.31}Fe_{0.17})_{\Sigma 1.03}$. This occupancy corresponds to 5.98 e^-, which agrees very well with findings from the crystal-structure refinement. It should be noted that there is quite a large degree of variation in these minor amounts of chemical constituents, but the average obtained for both chemical analyses and for crystal-structure analyses indicates that this site is only half-occupied. We do not understand the crystal-chemical ramifications of this result, but one explanation would be that the crystal structure might be in a lower-symmetry space group containing an atom site with a site multiplicity of 1. In terms of subgroups, this would indicate *P*2, but the present data are not sufficiently accurate to test this possibility, and there is really no other indication of monoclinic symmetry.

The polymerization of the borate polyhedra may be described as highly corrugated sheets on (010) (Figs. 5a, b). The wavelength of the corrugation is approximately 15 Å (*i.e.*, the *a* unit-cell length). The amplitude is approximately 5 Å (*i.e.*, 1/4 *b* unit-cell length). These corrugated sheets are cross-linked and re-inforced by *Ca* and *Mg* sites. The corrugations create large ovoid channels (7 × 14 Å) that parallel [001]. These channels contain the H_2O groups and Cl atoms. The sheet (Fig. 6a) consists of 17-membered rings with the rings stretched parallel to [001]. Within the 17-membered rings, triangular and tetrahedral borate polyhedra alternate with but one exception. The rings are decorated by two additional sets of polyhedra, a 3-membered ring, ⟨Δ2□⟩ and a 3-connected triangular polyhedron, [Δ] □|□|□|. The fundamental building block (FBB) for this ring is 12Δ14□:⟨Δ□Δ□ – [□]Δ|Δ|Δ| – [Δ]□|□|□| – ⟨Δ2□⟩•⟩

TABLE 2. WALKERITE: INFORMATION ON DATA COLLECTION AND STRUCTURE REFINEMENT

Simplified formula: $Ca_{16}(Mg,Li,\square)(B_{13}O_{17}(OH)_{12})_4Cl_4{\cdot}28H_2O$	
Space group: *Pba*2 (no. 32)	μ 0.97 mm^{-1}
Radiation: Mo*Kα*	Reflections collected: 28694
a 15.5484(6) Å	Unique reflections: 9001
b 22.6720(9) Å	Observed reflections ($> 4\sigma F_o$) 5420
c 8.7722(3) Å	Merged reflections: 3050
V 3092.3(3) Å^3	*Z* = 1
R(int) = 0.0807	Goof = 1.053 (all data)

$R = \Sigma(F_o - F_c) / \Sigma F_o = 0.042$ (for F_o), 0.088 (for all *F*) and 0.040 (for all *F* merged)

$wR^2 = [\Sigma w(F_o - F_c)^2 / \Sigma w(F_o)^2] = 0.097$ for $w = 0.0409$

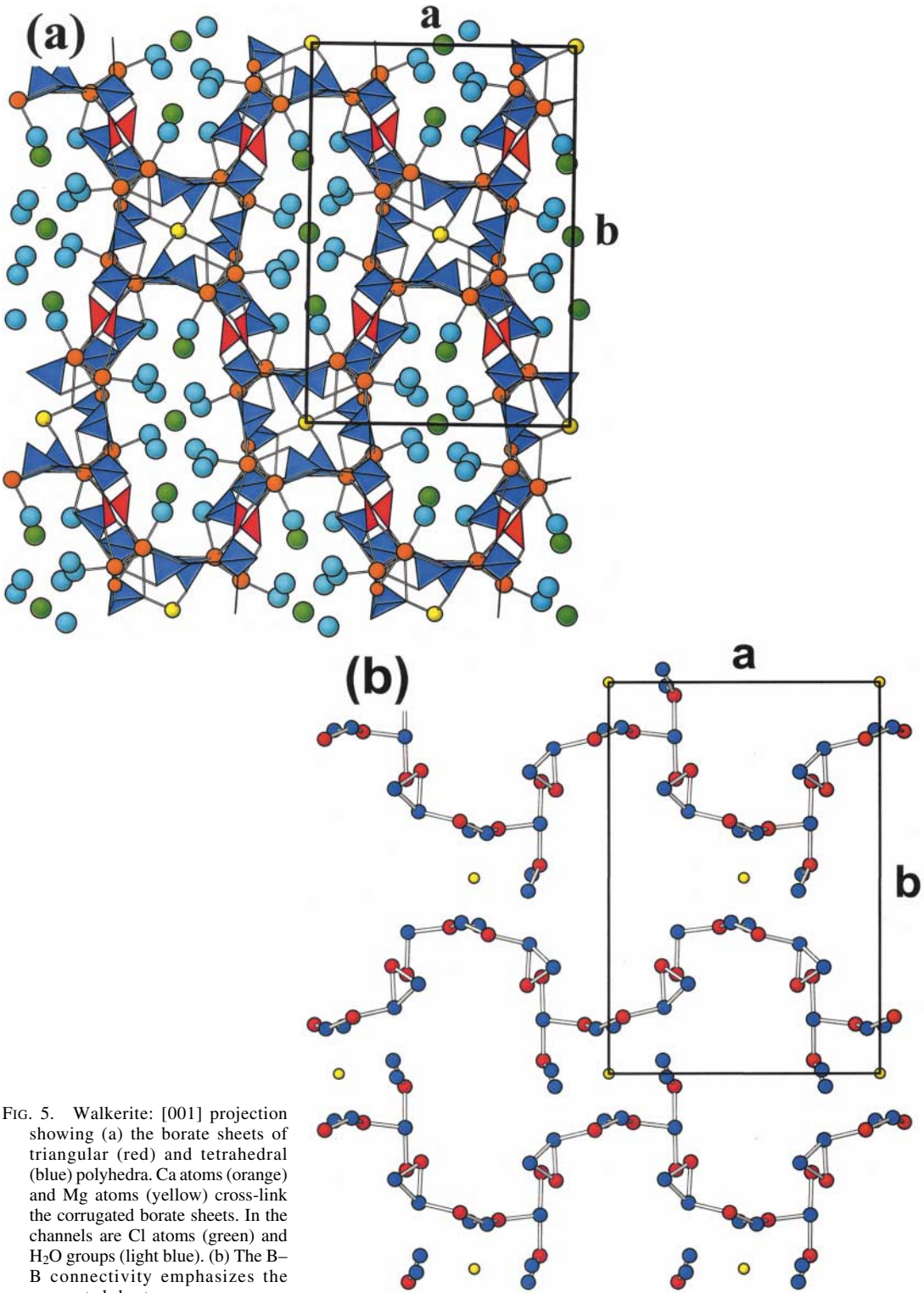

FIG. 5. Walkerite: [001] projection showing (a) the borate sheets of triangular (red) and tetrahedral (blue) polyhedra. Ca atoms (orange) and Mg atoms (yellow) cross-link the corrugated borate sheets. In the channels are Cl atoms (green) and H_2O groups (light blue). (b) The B–B connectivity emphasizes the corrugated sheets.

TABLE 3. WALKERITE: ATOM COORDINATES AND ANISOTROPIC DISPLACEMENT PARAMETERS (Å^3)

Site	x	y	z	U_{11}	U_{22}	U_{33}	U_{23}	U_{13}	U_{12}	U_{eq}
Ca1	0.22032(6)	0.11193(3)	0.6118(2)	0.0208(6)	0.0115(4)	0.0119(4)	-0.0004(4)	-0.0010(4)	0.0002(4)	0.0147(2)
Ca2	0.34082(6)	0.35920(4)	0.5024(2)	0.0158(5)	0.0148(4)	0.0107(4)	-0.0002(4)	0.0010(4)	-0.0016(4)	0.0137(2)
Ca3	0.23942(6)	0.41866(4)	0.1149(2)	0.0208(6)	0.0134(4)	0.0119(4)	-0.0007(4)	0.0014(5)	-0.0005(4)	0.0154(2)
Ca4	0.11625(6)	0.16220(4)	0	0.0152(5)	0.0300(5)	0.0106(4)	0.0026(4)	-0.0004(5)	-0.0032(4)	0.0186(2)
Mg1	0	0	0.0529(5)	0.0123(29)	0.0235(28)	0.0121(24)	0	0	-0.0023(20)	0.0160(16)
Cl1	0.5279(10)	0.19194(6)	0.6788(2)	0.0390(9)	0.0367(8)	0.0435(8)	-0.0089(6)	-0.0173(7)	0.0076(7)	0.0397(4)
Cl2	½	0	0.7865(3)	0.0509(16)	0.0477(13)	0.0350(12)	0	0	0.0187(11)	0.0445(6)
B1	0.2199(4)	0.0636(2)	0.2296(6)	0.0233(34)	0.0186(27)	0.0100(25)	0.0014(22)	0.0001(24)	-0.0010(25)	0.0173(12)
B2	0.1966(4)	0.2743(2)	0.2839(6)	0.0082(28)	0.0170(27)	0.0157(28)	0.0000(22)	0.0058(22)	-0.0018(22)	0.0136(11)
B3	-0.0898(4)	0.1253(2)	-0.1184(6)	0.0114(31)	0.0148(26)	0.0179(28)	0.0029(22)	-0.0013(24)	-0.0011(21)	0.0147(12)
B4	0.2565(3)	0.4665(2)	0.7296(6)	0.0107(29)	0.0141(26)	0.0157(26)	-0.0017(21)	-0.0014(23)	-0.0009(21)	0.0135(11)
B5	0.0526(4)	0.1447(2)	0.3820(6)	0.0160(33)	0.0176(25)	0.0152(27)	0.0007(23)	-0.0019(24)	0.0002(23)	0.0163(12)
B6	0.2510(4)	0.2540(2)	0.7454(6)	0.0164(32)	0.0153(26)	0.0126(25)	-0.0013(20)	-0.0066(23)	0.0014(22)	0.0148(12)
B7	0.2139(4)	-0.0086(2)	0.4565(6)	0.0212(34)	0.0189(27)	0.0084(25)	0.0005(20)	-0.0035(22)	0.0019(24)	0.0162(12)
B8	0.0168(4)	0.1215(2)	0.6546(6)	0.0121(30)	0.0237(27)	0.0080(25)	-0.0026(20)	-0.0013(21)	-0.0022(22)	0.0146(11)
B9	0.2559(4)	0.3619(2)	0.8098(6)	0.0238(33)	0.0122(25)	0.0048(22)	-0.0045(20)	0.0029(23)	-0.0032(23)	0.0136(11)
B10	0.2996(4)	0.5336(2)	-0.04700(6)	0.0380(42)	0.0114(26)	0.0132(27)	-0.0006(20)	-0.0023(26)	-0.0084(25)	0.0208(14)
B11	0.2938(4)	0.2290(2)	0.4775(6)	0.0225(32)	0.0109(23)	0.0112(28)	-0.0003(20)	0.0047(23)	0.0002(21)	0.0148(12)
B12	0.2046(4)	0.1692(2)	0.3044(6)	0.0149(33)	0.0161(27)	0.0102(24)	-0.0035(20)	-0.0046(22)	0.0026(22)	0.0138(12)
B13	-0.0472(4)	0.1141(3)	0.1636(6)	0.0118(31)	0.0373(33)	0.0117(26)	0.0067(24)	-0.0002(22)	0.0027(26)	0.0203(13)
O1	0.2100(2)	0.1221(1)	0.1917(3)	0.0232(20)	0.0095(15)	0.0104(16)	-0.0001(12)	0.0023(14)	0.0001(12)	0.0144(7)
O2	0.2239(2)	0.0480(1)	0.3786(4)	0.0343(23)	0.0177(16)	0.0100(16)	0.0022(14)	-0.0040(15)	-0.0010(15)	0.0206(8)
O3	0.2769(2)	0.5229(1)	0.1155(4)	0.0619(27)	0.0106(15)	0.0136(16)	-0.0008(16)	0.0049(19)	-0.0060(16)	0.0287(9)
O4	0.2432(2)	0.2800(1)	0.4134(3)	0.0222(19)	0.0109(15)	0.0101(16)	0.0008(12)	-0.0031(14)	0.0000(13)	0.0144(7)
OH5	0.1670(2)	0.3260(1)	0.2144(4)	0.0325(22)	0.0110(15)	0.0188(17)	0.0022(14)	-0.0053(16)	-0.0002(15)	0.0208(8)
O6	0.1797(2)	0.2219(1)	0.2161(4)	0.0171(18)	0.0082(14)	0.0137(15)	-0.0018(13)	-0.0022(14)	-0.0005(13)	0.0130(7)
O7	-0.1749(2)	0.1290(1)	-0.0791(3)	0.0133(19)	0.0170(16)	0.0156(18)	0.0006(12)	-0.0014(14)	0.0040(13)	0.0153(7)
O8	-0.0308(2)	0.1237(1)	-0.0016(4)	0.0135(18)	0.0370(19)	0.0088(14)	0.0006(16)	0.0041(16)	-0.0005(14)	0.0198(7)
O9	0.4333(2)	0.3774(1)	0.7328(4)	0.0149(18)	0.0278(19)	0.0096(16)	-0.0004(13)	0.0016(14)	0.0027(14)	0.0174(7)
O10	0.2574(2)	0.4837(1)	-0.1202(4)	0.0298(22)	0.0128(15)	0.0114(16)	0.0009(13)	0.0020(15)	-0.0041(14)	0.0180(7)
O11	0.2522(2)	0.4085(1)	0.6948(4)	0.0190(20)	0.0128(15)	0.0122(16)	0.0007(13)	-0.0001(14)	-0.0004(13)	0.0147(7)
O12	0.2399(2)	0.0065(1)	0.6136(4)	0.0222(18)	0.0127(14)	0.0116(14)	-0.0052(15)	-0.0034(16)	0.0009(12)	0.0155(6)
O13	0.1360(2)	0.1561(1)	0.4180(3)	0.0148(19)	0.0199(17)	0.0080(17)	0.0001(12)	0.0011(13)	-0.0009(13)	0.0142(7)
O14	0.0292(2)	0.1413(2)	0.2326(4)	0.0153(20)	0.0544(24)	0.0112(18)	0.0050(16)	-0.0022(15)	-0.0108(18)	0.0270(9)
O15	0.4948(2)	0.3639(1)	0.4973(4)	0.0139(18)	0.0259(17)	0.0115(15)	-0.0021(15)	-0.0033(16)	0.0032(13)	0.0171(7)
O16	0.2630(2)	0.2125(1)	0.6347(4)	0.0224(18)	0.0145(14)	0.0092(16)	0.0034(12)	0.0012(14)	-0.0026(13)	0.0154(7)
O17	0.2719(2)	0.3094(1)	0.7200(4)	0.0249(20)	0.0121(16)	0.0134(16)	0.0000(13)	0.0041(15)	-0.0030(14)	0.0168(7)
OH18	0.2183(2)	0.2339(1)	0.8847(4)	0.0343(23)	0.0222(17)	0.0150(17)	0.0016(14)	0.0058(17)	-0.0092(16)	0.0238(8)
OH19	0.2618(2)	-0.0575(1)	0.3844(4)	0.0304(21)	0.0169(17)	0.0126(16)	-0.0024(14)	-0.0013(16)	0.0004(14)	0.0200(7)
OH20	0.1238(2)	-0.0292(1)	0.4585(4)	0.0218(20)	0.0214(17)	0.0219(19)	-0.0026(14)	-0.0041(14)	-0.0044(15)	0.0217(8)
OH21	0.0794(2)	0.1625(1)	0.7270(4)	0.0180(19)	0.0307(19)	0.0107(16)	-0.0006(14)	-0.0023(15)	-0.0072(15)	0.0198(7)
OH22	0.0607(2)	0.0641(1)	0.6568(4)	0.0368(23)	0.0269(19)	0.0188(18)	0.0013(15)	-0.0016(16)	0.0111(16)	0.0275(8)
OH23	0.1785(2)	0.3596(1)	-0.0959(3)	0.0127(19)	0.0226(16)	0.0124(16)	0.0012(14)	0.0047(14)	-0.0022(14)	0.0159(7)
OH24	0.3924(3)	0.5324(2)	-0.0613(4)	0.0382(27)	0.0540(26)	0.0283(21)	0.0118(18)	-0.0015(18)	-0.0277(21)	0.0402(11)
OH25	0.2285(2)	0.0910(1)	0.8895(4)	0.0628(28)	0.0112(15)	0.0138(17)	0.0037(14)	-0.0018(19)	0.0072(17)	0.0292(9)
O26	0.2843(2)	0.1762(1)	0.3864(4)	0.0177(19)	0.0116(15)	0.0131(15)	-0.0033(13)	0.0000(14)	0.0005(13)	0.0141(7)
OH27	0.3806(2)	0.2530(1)	0.4801(4)	0.0128(17)	0.0199(16)	0.0225(19)	-0.0005(14)	-0.0001(15)	-0.0066(14)	0.0184(7)
OH28	0.3711(2)	0.3609(1)	0.2220(4)	0.0144(18)	0.0309(18)	0.0120(16)	0.0028(15)	0.0030(14)	0.0007(15)	0.0191(7)
OH29	0.4468(2)	0.4495(2)	0.1914(4)	0.0395(25)	0.0289(20)	0.0335(22)	-0.0067(18)	0.0086(18)	-0.0090(17)	0.0340(10)
OW1	0.0969(2)	0.4621(2)	0.1124(5)	0.0333(24)	0.0455(23)	0.0363(22)	0.0033(20)	0.0017(21)	0.0108(18)	0.0384(9)
OW2	0.0436(2)	0.2587(1)	0.0077(5)	0.0326(23)	0.0318(20)	0.0317(19)	0.0057(19)	0.0047(20)	0.0024(16)	0.0321(8)
OW3	0.3744(2)	0.0992(2)	0.6358(5)	0.0263(22)	0.0322(20)	0.0579(27)	0.0053(19)	-0.0040(21)	0.0024(17)	0.0388(10)
OW4	0.4277(2)	-0.0748(2)	0.4868(5)	0.0336(26)	0.0582(26)	0.0432(25)	0.0150(22)	-0.0006(22)	0.0054(20)	0.0450(10)
OW5	-0.1123(3)	0.2602(2)	0.1514(5)	0.0577(30)	0.0335(22)	0.0488(26)	0.0006(19)	0.0317(23)	0.0004(20)	0.0466(12)
OW6	0.0778(3)	0.5732(2)	0.2862(5)	0.0515(34)	0.1170(46)	0.0438(28)	-0.0224(28)	0.0006(24)	0.0134(31)	0.0707(16)
OW7	0.392(3)	0.1221(2)	0.9943(6)	0.0828(40)	0.0862(36)	0.0562(30)	-0.0005(32)	-0.0038(32)	-0.0251(30)	0.0751(15)

(Burns *et al.* 1995). This FBB is translated once (*i.e.*, symbol •) to form the 17-membered, S-shaped ring (Fig. 6b). A similar, but not identical, channel is found in the structures of pringleite and ruitenbergite (Grice *et al.* 1994) and penobsquisite (Grice *et al.* 1996). Borate minerals with FBBs of this magnitude are sparse in number (Grice *et al.* 1999). Among structures of the borate minerals, the only ones with FBBs greater than six are:

TABLE 4. WALKERITE: SELECTED BOND LENGTHS (Å) AND ANGLES (°)

Ca1-O13	2.369(3)	Ca2-O15	2.397(3)	Ca3-O7	2.416(3)	Ca4-O1	2.404(3)
Ca1-O16	2.383(3)	Ca2-O11	2.448(3)	Ca3-OW1	2.424(4)	Ca4-O8	2.447(3)
Ca1-O12	2.410(3)	Ca2-O17	2.462(3)	Ca3-OH19	2.426(3)	Ca4-OH21	2.463(3)
Ca1-OW3	2.423(4)	Ca2-O4	2.478(3)	Ca3-O3	2.434(3)	Ca4-OW2	2.464(3)
Ca1-OH25	2.485(3)	Ca2-OH27	2.492(3)	Ca3-OH23	2.472(3)	Ca4-OH18	2.486(3)
Ca1-O2	2.507(3)	Ca2-OH28	2.505(3)	Ca3-OH5	2.539(3)	Ca4-O14	2.494(3)
Ca1-O26	2.650(3)	Ca2-O9	2.514(3)	Ca3-O10	2.550(3)	Ca4-O6	2.529(3)
Ca1-OH21	2.672(3)	Ca2-OH20	2.619(3)	Ca3-OH28	2.605(3)	Ca4-OH25	2.566(4)
Ca1-OH22	2.737(4)	Ca2-OH19	2.680(3)			Ca4-OH24	2.994(4)
⟨Ca1-O⟩	2.515	⟨Ca2-O⟩	2.510	⟨Ca3-O⟩	2.483	⟨Ca4-O⟩	2.538
Mg-OH29	1.863(4)x2	OH29-OH29[1]	98.6(3)				
Mg-OH24	2.085(5)x2	OH29-OH24	116.9(2)x2				
⟨Mg-O⟩	1.974	OH29-OH24[1]	100.0(2)x2				
		OH24-OH24[1]	122.5(3)				
		⟨O-Mg-O⟩	109.5				
B1-O2	1.356(6)	O2-O3	122.0(4)	B2-O4	1.353(6)	O4-O6	123.8(4)
B1-O3	1.362(6)	O2-O1	119.3(4)	B2-O6	1.355(6)	O4-OH5	117.6(4)
B1-O1	1.375(6)	O3-O1	118.6(4)	B2-OH5	1.398(6)	O6-OH5	118.6(4)
⟨B1-O⟩	1.364	⟨O-B1-O⟩	120.0	⟨B2-O⟩	1.369	⟨O-B2-O⟩	120.0
B3-O9	1.355(6)	O9-O7	120.1(4)	B4-O11	1.353(6)	O11-O12	118.7(4)
B3-O7	1.370(6)	O9-O8	122.6(4)	B4-O12	1.363(6)	O11-O10	119.5(4)
B3-O8	1.376(6)	O7-O8	117.2(4)	B4-O10	1.374(6)	O12-O10	121.8(4)
⟨B3-O⟩	1.367	⟨O-B3-O⟩	120.0	⟨B4-O⟩	1.363	⟨O-B4-O⟩	120.0
B5-O13	1.360(6)	O13-O14	119.2(4)	B6-O17	1.318(6)	O17-O16	120.3(4)
B5-O14	1.363(6)	O13-O15	118.9(4)	B6-O16	1.364(6)	O17-OH18	123.2(4)
B5-O15	1.367(6)	O14-O15	121.8(4)	B6-OH18	1.400(6)	O16-OH18	116.5(4)
⟨B5-O⟩	1.363	⟨O-B5-O⟩	120.0	⟨B6-O⟩	1.361	⟨O-B6-O⟩	120.0
B7-O2	1.462(6)	O2-O12	101.8(4)	B8-O15	1.459(6)	O15-O9	103.3(4)
B7-O12	1.476(6)	O2-OH20	112.6(4)	B8-O9	1.468(6)	O15-OH22	108.7(4)
B7-OH20	1.477(6)	O2-OH19	113.9(4)	B8-OH22	1.470(6)	O15-OH21	114.6(4)
B7-OH19	1.478(6)	O12-OH20	108.8(4)	B8-OH21	1.488(6)	O9-OH22	114.8(4)
⟨B7-O⟩	1.473	O12-OH19	115.8(4)	⟨B8-O⟩	1.471	O9-OH21	111.6(4)
		OH20-OH19	104.2(4)			OH22-OH21	104.1(4)
		⟨O-B7-O⟩	109.5			⟨O-B8-O⟩	109.5
B9-O17	1.448(6)	O17-O11	103.0(3)	B10-OH24	1.447(8)	OH24-O10	113.4(4)
B9-O11	1.461(6)	O17-OH23	114.8(4)	B10-O10	1.458(6)	OH24-OH25	106.1(4)
B9-OH23	1.462(6)	O17-O7	110.6(4)	B10-OH25	1.483(6)	OH24-O3	108.5(4)
B9-O7	1.467(6)	O11-OH23	112.6(6)	B10-O3	1.488(6)	O10-OH25	112.5(4)
⟨B9-O⟩	1.460	O11-O7	112.7(6)	⟨B10-O⟩	1.469	O10-O3	100.9(4)
		OH23-O7	103.4(3)			OH25-O3	115.6(4)
		⟨O-B9-O⟩	109.517			⟨O-B10-O⟩	109.5
B11-O26	1.448(6)	O26-OH27	114.4(4)	B12-O26	1.441(6)	O26-O1	111.7(4)
B11-OH27	1.455(6)	O26-O4	112.0(4)	B12-O1	1.458(6)	O26-O6	113.4(4)
B11-O4	1.506(6)	O26-O16	105.5(4)	B12-O6	1.477(6)	O26-O13	107.7(4)
B11-O16	1.507(6)	OH27-O4	101.7(3)	B12-O13	1.489(6)	O1-O6	104.6(4)
⟨B11-O⟩	1.479	OH27-O16	111.9(4)	⟨B12-O⟩	1.466	O1-O13	110.4(4)
		O4-O16	111.5(4)			O6-O13	108.9(4)
		⟨O-B11-O⟩	109.5			⟨O-B12-O⟩	109.4
B13-OH29	1.464(7)	OH29-O14	113.4(4)	Cl1-OW2	3.105(4)	Cl2-OW3	3.258(4)x2
B13-O14	1.469(7)	OH29-OH28	105.4(4)	Cl1-OW3	3.203(4)	Cl2-OW4	3.324(5)x2
B13-OH28	1.482(7)	OH29-O8	108.6(4)	Cl1-OW4	3.220(4)	Cl2-OW1	3.344(4)x2
B13-O8	1.488(6)	O14-OH28	112.9(4)				
⟨B13-O⟩	1.476	O14-O8	101.5(4)	OW5-OW2	2.731(5)	OW6-OW4	2.924(6)
		OH28-O8	115.3(4)	OW5-OH28	2.826(5)	OW6-OW1	2.960(6)
		⟨O-B13-O⟩	109.5	OW5-OH27	2.901(5)	OW7-OH25	2.793(6)
						OW7-OW6	2.829(7)

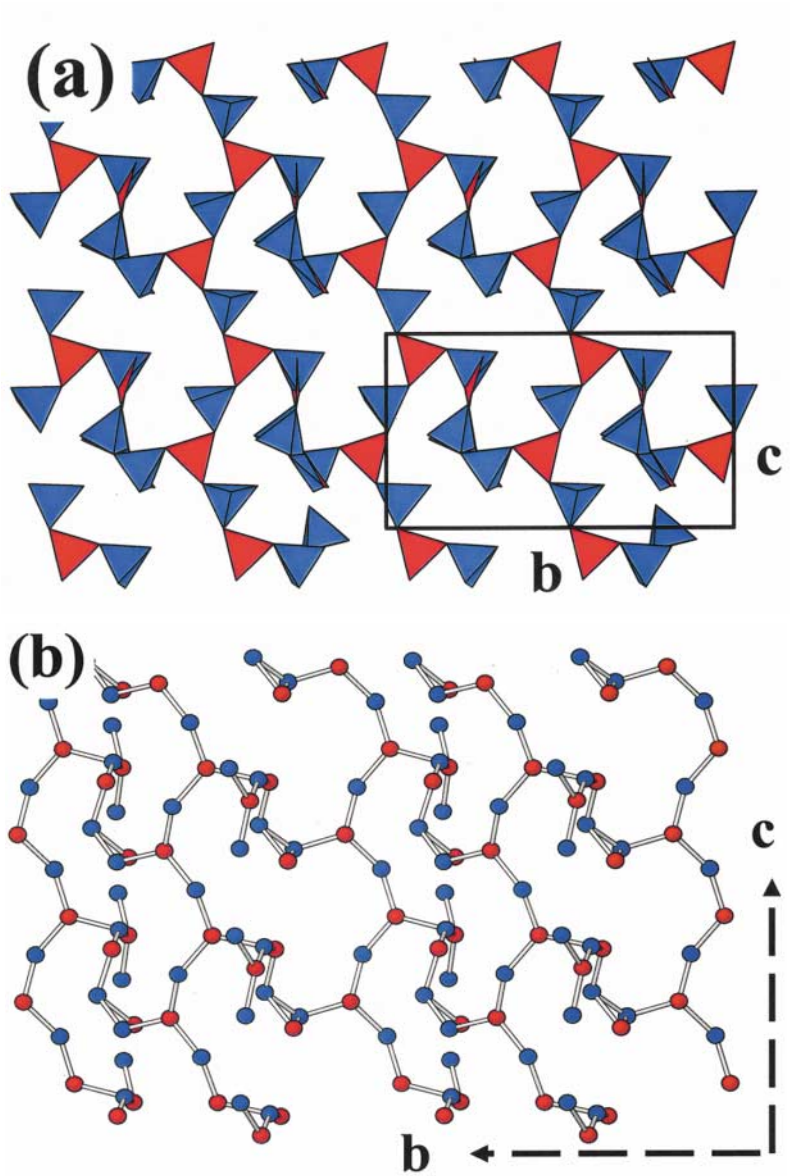

FIG. 6. Walkerite: (010) borate sheet of 17-membered rings: FBB: 12Δ14□:⟨Δ□Δ□ – [□]Δ□|Δ□|Δ□| – [Δ]□|□|□| – ⟨Δ2□⟩•⟩. (a) Borate polyhedra, (b) B–B connectivity, characterized by large "S"-shaped channels (inclined view).

kernite with a chain structure, strontioborite, ginorite, johachidolite and preobrazhenskite with sheet structures, and the boracite series (boracite, chambersite, congolite, ericaite and trembathite), pringleite, ruitenbergite and penobsquisite with framework structures. All of these minerals, except johachidolite, have within their structure the very common three-membered ring of boron polyhedra (Burns *et al.* 1995). Pringleite, ruitenbergite and penobsquisite are unique in that they are the only examples of structures with twelve-membered rings of borate polyhedra.

Schindler & Hawthorne (2001) have formulated a method to determine the conditions of formation of borate minerals. They have calculated the topology of a

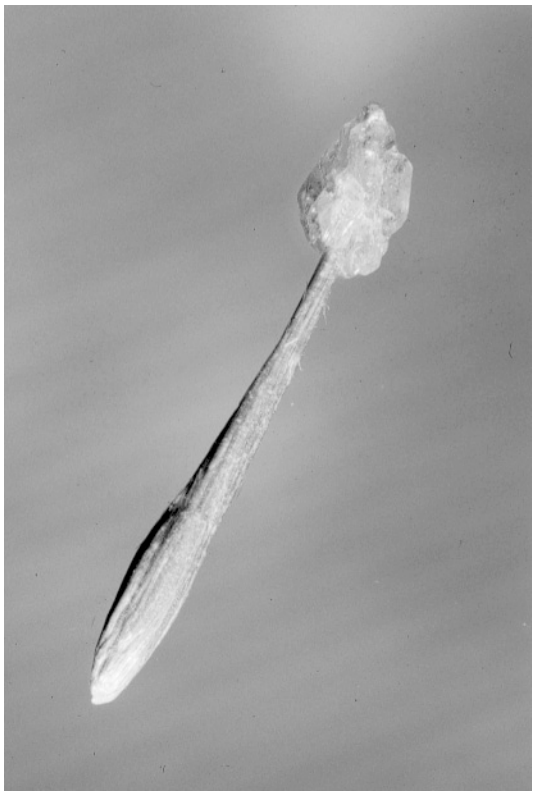

Photograph of a bundle of walkerite fibers 6 mm in length, capped by hilgardite. Photograph by Q. Wight.

pH – log[H_2O] diagram incorporating each of the borate structural units. Overlain on this topology, they have constructed two additional figures using the parameters: (a) average basicity (AB), and (b) percentage of tetrahedrally coordinated B ($^{[4]}$B). For the mineral assemblage we are discussing from Sussex, the AB (*vu*) and $^{[4]}$B (%) for each mineral is: walkerite (0.23, 54), volkovskite (0.23, 33), hilgardite (0.33, 60), hydroboacite (0.37, 67), boracite (0.38, 86) and szaibelyite (0.71, 0). If we apply these numbers to the relevant pH – log[H_2O] activity–activity diagram, almost the entire range of pH and log[H_2O] is covered. This seems highly unlikely considering the close association of these minerals within the occurrence.

Walkerite provides yet another example of the complex polymerization present in sequences of marine evaporites. Grice *et al.* (1994) attributed this structural complexity to the presence of Cl^- anions, but it is also known that the Sussex deposits have been intensely folded (Waugh & Urquhart 1983). It is premature to speculate on a possible correlation between grade of metamorphism and the development of highly polymerized structures within the borate minerals.

Acknowledgements

The authors gratefully acknowledge the cooperation of, and samples provided by, Mr. Brian Roulston, Potash Corporation of Saskatchewan (New Brunswick Division). The authors are indebted to Dr. Alf Olav Larsen and Mrs. Ingmarie Vedaa, Norsk Hydro ASA, Research Centre Porsgrunn, for the TGA analysis and to Elizabeth Moffatt, Canadian Conservation Institute, for the infrared spectrum. We thank Dr. Lee Groat, University of British Columbia, for the use of the four-circle diffractometer, and Quintin Wight for the photograph of walkerite. Helpful comments from the referee, Dr. Dmitry Pushcharovsky, Associate Editor, Dr. Vladimir Bermanec and from the Editor, Dr. Robert F. Martin, improved the quality of the manuscript.

References

Burns, P.C., Grice, J.D. & Hawthorne, F.C. (1995): Borate minerals. I. Polyhedral clusters and fundamental building blocks. *Can. Mineral.* **33**, 1131-1151.

_____, Hawthorne, F.C. & Stirling, J.A.R. (1992): Trembathite, $(Mg,Fe)_3B_7O_{13}Cl$, a new borate mineral from the Salt Springs potash deposit, Sussex, New Brunswick. *Can. Mineral.* **30**, 445-448.

Farmer, V.C. (1974): *The Infrared Spectra of Minerals*. Mineralogical Society, London, U.K.

Grice, J.D., Burns, P.C. & Hawthorne, F.C. (1994): Determination of the megastructures of the borate polymorphs pringleite and ruitenbergite. *Can. Mineral.* **32**, 1-14.

_____, _____ & _____ (1999): Borate minerals. II. A hierarchy of structures based upon the borate fundamental building block. *Can. Mineral.* **37**, 731-762.

_____, Gault, R.A. & Van Velthuizen, J. (1996): Penobsquisite: a new borate mineral with a complex framework structure. *Can. Mineral.* **34**, 657-665.

_____, _____ & _____ (1997): Brianroulstonite: a new borate mineral with a sheet structure. *Can. Mineral.* **35**, 751-758.

Ibers, J.A. & Hamilton, W.C., eds. (1974): *International Tables for X-ray Crystallography* IV. The Kynoch Press, Birmingham, U.K.

Mandarino, J.A. (1981): The Gladstone–Dale relationship. IV. The compatibility concept and its application. *Can. Mineral.* **19**, 441-450.

Ondik, H. & Smith, S. (1968): *International Tables for X-ray Crystallography* III. The Kynoch Press, Birmingham, U.K.

ROBERTS, A.C., STIRLING, J.A.R., GRICE, J.D., BURNS, P.C., ROULSTON, R.V., CURTIS, J.D. & JAMBOR, J.L. (1993): Pringleite and ruitenbergite, polymorphs of $Ca_9B_{26}O_{34}(OH)_{24}Cl_4 \bullet 13H_2O$, two new mineral species from Sussex, New Brunswick. *Can. Mineral.* **31**, 795-800.

ROULSTON, B.V. & WAUGH, D.C.E. (1981): A borate mineral assemblage from the Penobsquis and Salt Springs evaporite deposits of southern New Brunswick. *Can. Mineral.* **19**, 291-301.

SCHINDLER, M. & HAWTHORNE, F.C. (2001): A bond-valence approach to the structure, chemistry and paragenesis of hydroxyl-hydrated oxysalt minerals. III. Paragenesis of borate minerals. *Can. Mineral.* **39**, 1257-1274.

WAUGH, D.C.E. & URQUHART, B.R. (1983): The geology of Denison–Potacan's New Brunswick potash deposit. *Proc. Sixth Int. Symp. on Salt*, 85-98.

Received February 2, 2002, revised manuscript accepted September 26, 2002.